




Zoledronate and Molecular Iodine Cause Synergistic Cell Death in Triple Negative Breast Cancer through Endoplasmic Reticulum Stress

Ranu Tripathi, Preeti Singh, Aru Singh, Megha Chagtoo, Sajid Khan, Swasti Tiwari, Gaurav Agarwal, Syed Musthapa Meeran & Madan M Godbole

To cite this article: Ranu Tripathi, Preeti Singh, Aru Singh, Megha Chagtoo, Sajid Khan, Swasti Tiwari, Gaurav Agarwal, Syed Musthapa Meeran & Madan M Godbole (2016): Zoledronate and Molecular Iodine Cause Synergistic Cell Death in Triple Negative Breast Cancer through Endoplasmic Reticulum Stress, *Nutrition and Cancer*, DOI: [10.1080/01635581.2016.1158293](https://doi.org/10.1080/01635581.2016.1158293)

To link to this article: <http://dx.doi.org/10.1080/01635581.2016.1158293>

 View supplementary material 

 Published online: 26 Apr 2016.

 Submit your article to this journal 

 View related articles 

 View Crossmark data 

Zoledronate and Molecular Iodine Cause Synergistic Cell Death in Triple Negative Breast Cancer through Endoplasmic Reticulum Stress

Ranu Tripathi^a, Preeti Singh^a, Aru Singh^b, Megha Chagtoo^b, Sajid Khan^c, Swasti Tiwari^b, Gaurav Agarwal^d, Syed Musthapa Meeran^c, and Madan M Godbole^{a,b}

^aDepartment of Endocrinology, Sanjay Gandhi Postgraduate Institute of Medical Sciences, Raebareli Road, Lucknow, India; ^bDepartment of Molecular Medicine and Biotechnology, Sanjay Gandhi Postgraduate Institute of Medical Sciences, Raebareli Road, Lucknow, India; ^cDepartment of Endocrine Surgery, Sanjay Gandhi Postgraduate Institute of Medical Sciences, Raebareli Road, Lucknow, India; ^dDepartment of Endocrinology, Central Drug Research Institute, Lucknow, India

ABSTRACT

Women consuming molecular iodine (I₂) through seaweeds suffer the least from breast cancers. Zoledronate (Zol) is in clinical use for alleviation of bone pain in cancer patients. Triple negative breast cancers exhibit high mortality due to lack of neoadjuvant chemotherapy. I₂ and Zol independently cause weak antiproliferative and apoptotic effect. So far, their combined effects have not been tested. We analyzed the effect of combination of I₂ with Zol as a potent adjuvant therapeutic agent for triple negative breast cancer cells (MDA-MBA-231) and in the mice model of breast cancer. Cell viability, terminal deoxynucleotidyl transferase dUTP nick end labeling staining, Western blotting, real-time PCR, flow cytometry, and other assays were performed for assessing cell death, calcium levels, and migration potential, respectively, in treated cells. The increased caspase 8, increased [Ca²⁺]_i levels, and endoplasmic reticulum (ER) stress resulted in apoptosis. Real time and fluorescence-based analysis demonstrated that the combination treatment targets ER Ca²⁺ homeostasis chaperons leading to apoptosis. Combination therapy reduces metalloproteinases 2 and 9, inhibits invasion/migration of cells, and prevents growth of tumor in mice.

I₂ + Zol combination treatment induces synergistic increase in ER-mediated apoptosis, reduces invasion/migration potential of MDA-MB-231 cells, and exhibits antiproliferative property in vivo demonstrating its potential as combination therapy.

ARTICLE HISTORY

Received 22 April 2015



Accepted 19 January 2016

Introduction

Evidence from field studies and results in animal models has strengthened the postulate that iodine plays an important role in breast physiology and has a protective role in breast cancer (1–4). This concept was reinforced by findings of low incidences of breast cancer and cardiovascular disease in populations consuming seaweeds, such as wakame, nori, and mekabu that contain high quantities of iodine in several chemical forms (5). In mammary gland, supplementation with molecular iodine (I₂), but not iodide (I⁻), alleviates human mastalgia, exerts potent antineoplastic and apoptotic effects on animal and human cancer (6). The mechanisms suggested for its protective role include modulation of estrogen pathway (7), indirect effect through iodolipid formation (8), antioxidant properties such as ROS scavenging and neutralizing OH radical (9), as well as loss of

mitochondrial membrane potential, thereby triggering mitochondrial-mediated apoptosis (10). In spite of an ambiguity about the exact mechanism of the cytotoxic action of I₂ on breast neoplasms, efforts are on to explore its further potential (11,12). In search for such an add-on, we hypothesized that the propensity of zoledronate (Zol) to protect bone loss in postmenopausal women, who are more prone to develop breast neoplasms, and its weak apoptotic property seen in cancer cells (13,14) may provide for antineoplastic adjuvancy in combination with I₂.

In the present work, we describe I₂ and Zol as an effective combination for triple negative breast cancers. We provide in vitro and in vivo evidence to show the ability of this combination to enhance cytotoxic effect as well as to induce apoptosis in triple negative breast cancer cells.

CONTACT Madan M Godbole  madangodbole@yahoo.co.in  Department of Endocrinology and Molecular Medicine and Biotechnology, Sanjay Gandhi Postgraduate Institute of Medical Sciences, Raebareli Road, Lucknow 226 014, India.

Color versions of one or more of the figures in the article can be found online at www.tandfonline.com/hnuc.

© 2016 Taylor & Francis Group, LLC

Materials and methods

Reagents and antibodies

We procured protease inhibitor mixture, iodine, potassium iodide, propidium iodide (PI), JC1 mitochondrial membrane potential dye (JC1), thapsigargin, ethylene glycol tetra acetic acid (EGTA), heparin, and RNase A from Sigma; BAPTA-AM, Fluo 3-AM, Oregon green BAPTA-AM, and cell culture reagents from Invitrogen; and antibodies against caspases-3, 8, and 12, Bax, Bcl₂, GADD153, GRP78, β -actin, and secondary antibodies from Cell Signaling Technology (MA, USA). Specific caspase inhibitors Z-1ETD-FMK and Z-VAD-FMK were purchased from R&D systems (Minneapolis, MN, USA). Zoledronic acid was a kind gift from Natco Pharmaceuticals, India.

Cell culture and viability assay

Human breast cancer cell lines, namely MCF-7, MDA-MB-231, MDA-MB-453, ZR-75-1, and T-47D (National Centre of Cell Sciences, Pune, India) were cultured in Dulbecco Modified Eagle Medium (DMEM) + F-12 medium containing 10% Fetal Bovine Serum (FBS) [12]. Cells were treated either with vehicle, I₂ (1–4 μ M), Zol (10–80 μ M), or I₂ (2 μ M) plus Zol (20 μ M) combination. The cytotoxic effect was analyzed using the trypan blue dye exclusion method.

Detection of apoptosis

To analyze apoptotic fractions after defined treatment, the cells were harvested and fixed in 70% ethanol at -20°C . Pelleted cells were stained for 1 h in 0.5 ml of staining solution (0.1 mg/ml RNase A in PBS, 0.5% (v/v) Triton X-100, and 40 μ g/ml PI). Fluorescence intensity of PI-stained DNA was detected in FL-2 (617 nm) mode in FACScan (Becton Dickinson Advanced Cellular Biology). DNA fragmentation and TUNEL (Roche Diagnostics) staining were performed as described previously (10,12). Cells were visualized using Nikon Eclipse 80i fluorescence microscope (Kawasaki, Japan).

Measurement of $\Delta\Psi_m$

The ampholytic cationic fluorescent probe, JC-1 stain, was used to monitor mitochondrial transmembrane potential using FACSCalibur flow cytometer (Becton Dickinson, San Jose, CA). JC-1 was excited at 530 nm, and fluorescence was analyzed at 527 nm (FL-1) and 590 nm (FL-2) after logarithmic amplification. Mitochondrial membrane potential is shown as a ratio of FL2/FL1 intensity.

Western blotting

Western blotting was performed as described previously (10,12). Membranes were reprobed with β -actin as a loading control.

RNA extraction and analysis

qPCR from total RNA was performed using SYBR Green chemistry using primer pairs (Supplementary Table 1). 2^{-ddCt} method was used for analysis. For quantification of X-box-binding protein 1 (Xbp1) splice variant, reaction products were analyzed by electrophoresis on 1.5% agarose followed by ethidium bromide staining.

Assay for measuring free cytosolic calcium [Ca^{2+}]

Free cytosolic calcium [Ca^{2+}]_c was measured by observing the intake of cell-permeant, Ca^{2+} -sensitive fluorescent dye Oregon green by cells in suspension using flow cytometry (520 nm, FL-1). Loading of heparin inside the cells to inhibit inositol-1,4,5-triphosphate receptor (IP3R)-mediated Ca^{2+} release was performed by cytoplasmic hypoosmotic pinocytotic lysis procedure (15). Briefly, cells were incubated in hypertonic solution for 5 min in MEM to form heparin-containing pinocytotic vesicles. Cells were exposed to hypoosmotic media for 2 min to promote pinocytotic lysis and the distribution of heparin throughout the cytoplasm. This procedure resulted in the loading of $\sim 90\%$ cells as determined by cytoplasmic localization of fluorescent fluorescein isothiocyanate-dextran, and did not contribute to cell toxicity (data not shown).

Fluorescence Ca^{2+} measurements in intact cells

For the Ca^{2+} measurements in intact cells, MDA-MB-231 cells were seeded in 96-well plates (density of approximately 5×10^5 cells/ml). Cells were pretreated with 1 mM EGTA before treatment with 10 μ M thapsigargin. This was followed by treatment with Zol+I₂. After the treatment, the cells were loaded for 30 min with 4 μ M Fluo 3-AM at 25°C in modified Krebs solution. Fluorescence was monitored on a microplate reader (Biotek) by alternately exciting the Ca^{2+} indicator at 480 nm and collecting emission fluorescence at 540 nm.

Wound-healing assay

In confluent monolayer culture, wounds were made using 200- μ l pipette tip by making a straight scratch, which stimulated a wound. The scratch was made by keeping the pipette tip at an angle of around 30° . Then the medium was

replaced by fresh complete medium (16). Wound healing as a function of cell migration across the wound was measured by determining the distances between the wound edges at 0, 12, and 24 h and photographs were taken (40X).

Invasion assay

For this assay, we used BD Biocoat™ Matrigel® Invasion chamber containing BD Falcon™ TC companion plate (17). We followed the assay protocol provided by the manufacturer (www.bdbiosciences.com). Migrating cells (lower surface of the membrane) were stained with methylene blue, photographed (40x), and counted in 5 randomly selected fields.

4T1-Syngeneic breast tumor model

All studies were conducted under approved protocol by the Institutional Animal Ethics Committee of the Central Drug Research Institute (CDRI). Approximately 1×10^6 4T1 cells were injected subcutaneously in the mammary fat pad of the right mammary gland of female Balb/c mice. Iodine was dissolved with potassium iodide (1:2) in double-distilled water. The amount of I_2 was estimated using the sodium thiosulfate titration method, and the stock solution of $75 \mu\text{M}$ (20.0 mg/L) I_2 was prepared. One week after the injection of 4T1 cells, the animals were randomly assigned to two groups (n-6). Zol (100 $\mu\text{g}/\text{kg}$ body weight) and Iodine (0.25 mg/kg body weight) were administered via intraperitoneal and oral routes, respectively. Control group animals were administered vehicles. The body weight and tumor size were measured every week. The tumor volume was calculated using the formula: $(L \times W^2) \times 0.5$, where L is the tumor length and W is tumor width (18).

Statistical analysis

Two-tailed Student's *t*-test and ANOVA followed by Bonferroni's method were used for two groups and multiple group comparisons, respectively. Data are presented as mean \pm SEM. *P* values of 0.05 were considered statistically significant.

Results

Combination of Zol and I_2 at suboptimal dose causes significant cell death of breast cancer cells

MDA-MB-231 cells exposed either to 80 μM Zol or 3 μM I_2 for 48 h induced cell death to the extent of 50–60% (Fig. S1 A, B). We empirically selected a dose of I_2 at 2 μM , wherein cell viability was still persistent at >60%; and a dose of Zol at 20 μM , wherein cell viability was not

different from that with untreated cells for combination therapy. The combined doses of Zol+ I_2 at 20 μM + 2 μM for 48 h cause >60% cell death of MDA-MB-231 cells (Fig. S1C). Further we confirmed that this combination dose resulted in significant cytotoxicity in various breast cancer cell lines, namely MCF-7, MDA-MB-231, and MDA-MB-468, when compared to treatment with Zol or I_2 alone (Fig. S1C). However, the cytotoxic effect of combination dose was found to a lesser extent in ZR-75 and TD47D (Fig. S1C). Once it is validated that this combination dose causes significant cell death (>60%) in MDA-MB-231 cells, providing a rationale for use of this combination dose in all other experiments.

Zol+ I_2 combination treatment of MDA-MB-231 cells for 48 h causes apoptotic cell death

It was observed that cells when treated with Zol+ I_2 for a period of 48 h show significantly increased time-dependent DNA fragmentation, hypodiploidy, and TUNEL positivity when compared to either vehicle-treated cells or cells treated separately with Zol or I_2 (Fig. 1A, 1B and 1C). The increased apoptosis appeared to be in proportion to the increased cytotoxicity (Fig. 1D).

Zol+ I_2 treatment causes mitochondria-independent apoptosis in MDA-MB-231 cells

Cells when treated with Zol+ I_2 showed no significant change in expression of both mitochondrial Bcl2 or Bcl-xl and cytosolic cytochrome C (Fig. 2A and 2B). Zol+ I_2 treatment caused no change in mitochondrial permeability as indicated by ratio of FL2/FL1 using JC-1 dye (Fig. 2C and 2D). On the contrary, there was a significant increase in caspase 3 and caspase 8 compared to vehicle or their individual treatments (Zol or I_2), which was inhibited by their specific inhibitors, Z-VAD-FMK and Z-1ETD-FMK (Fig. 2E–H), respectively.

Thus, apoptosis caused by Zol+ I_2 does not appear to be mediated by intrinsic mitochondrial mechanisms. However, extrinsically induced caspase 8 rise was insufficient to explain synergistic rise in apoptosis. Significantly increased protein levels of caspase 12 in I_2 -treated cells and Zol+ I_2 -treated cells relative to totally absent levels in vehicle or Zol alone (Fig. 2I, J) hinted at combination treatment causing enhanced endoplasmic reticulum (ER) stress as a plausible reason for caspase 12-mediated apoptosis.

Molecular iodine (I_2) increases $[Ca^{2+}]_c$ and ER stress

After 48 h of treatment, a significant increase in cytosolic $[Ca^{2+}]_c$ was observed in I_2 (2 μM)-treated cells

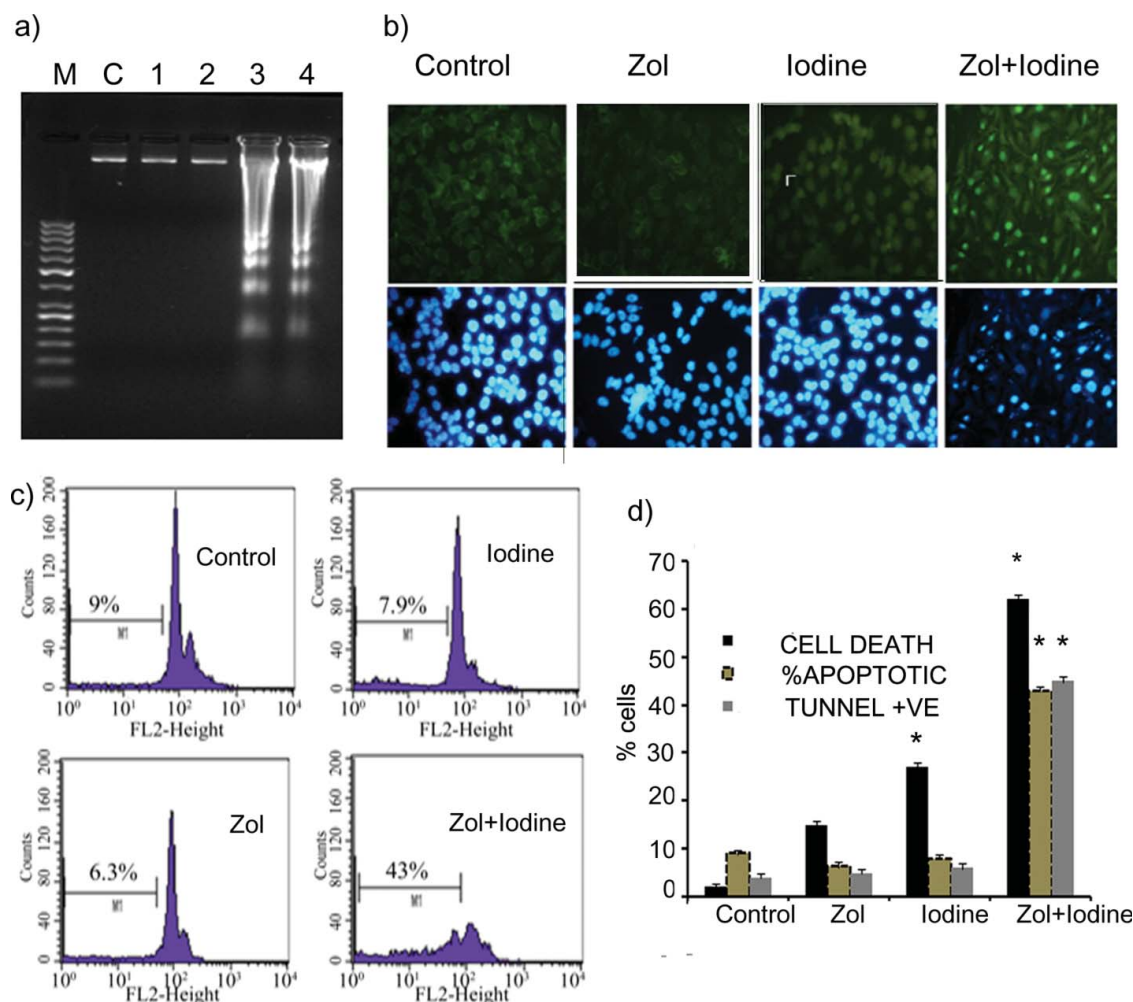


Fig.1

Figure 1. A: MDA-MB-231 cells were treated with vehicle, Zol, I₂, and Zol+I₂ at concentrations given in experimental design for 48 h, and 5 μ M staurosporine was the positive control (only for fragmentation). DNA was isolated and the ladder formation was examined on 1.8% agarose gel electrophoresis and fragmentation lanes described in the same order as per treatment modalities mentioned earlier. Vehicle treatment results are depicted as control denoted by C. B: Representative fluorescence micrograph (40X) of TUNEL-stained cells treated with the indicated treatments. C: Flow cytometric analysis of cells treated as above and then quantified for their DNA content after PI staining. Values shown in boxes are the % of cells with hypodiploid DNA. D: Histogram represents the sub-G1 fraction (%), the proportion of apoptotic cells, % cell death, and number of TUNEL-positive cells. The % of viable cells is expressed as mean \pm SD of triplicate experiment. * indicates $P < 0.01$ versus control.

compared to vehicle as indicated by increased intensity of Oregon green BAPTA dye (Fig. 3A). Chelating calcium using BAPTA (cell permeable), EGTA, or heparin resulted in [Ca²⁺]_c inhibition in I₂-treated cells (Fig. 3A). Meanwhile, blocking IP3R using heparin completely abolished the I₂-induced increase in [Ca²⁺]_c. Moreover, mRNA levels of IP3R3, GRP78, and spliced variant of Xbp1 were significantly increased in I₂-treated cells relative to vehicle (Fig. 3B, C, D)). Furthermore, a time course study showed an increase in GRP78 protein levels at an earlier time point (6 hours) than LC3 (24 hours) in I₂-treated cells (Fig. S1D, E). The overall results indicate

that I₂ in MDA-MB-231 cells resulted in IP3R-mediated increase in [Ca²⁺]_c and ER stress.

Apoptosis caused by combination treatment is due to pronounced [Ca²⁺]_c changes and ER stress involving molecular chaperons

Measurement of cytosolic Ca²⁺ indicated significant increase of [Ca²⁺]_c (Fig. 4A) as well as hypodiploidy (Fig. 4B) in cells treated with Zol+I₂ compared to vehicle-treated cells. Moreover, as observed with I₂ alone, heparin completely inhibited [Ca²⁺]_c in Zol+I₂-treated cells (Fig. 4A). Hypodiploidy was also significantly reduced in

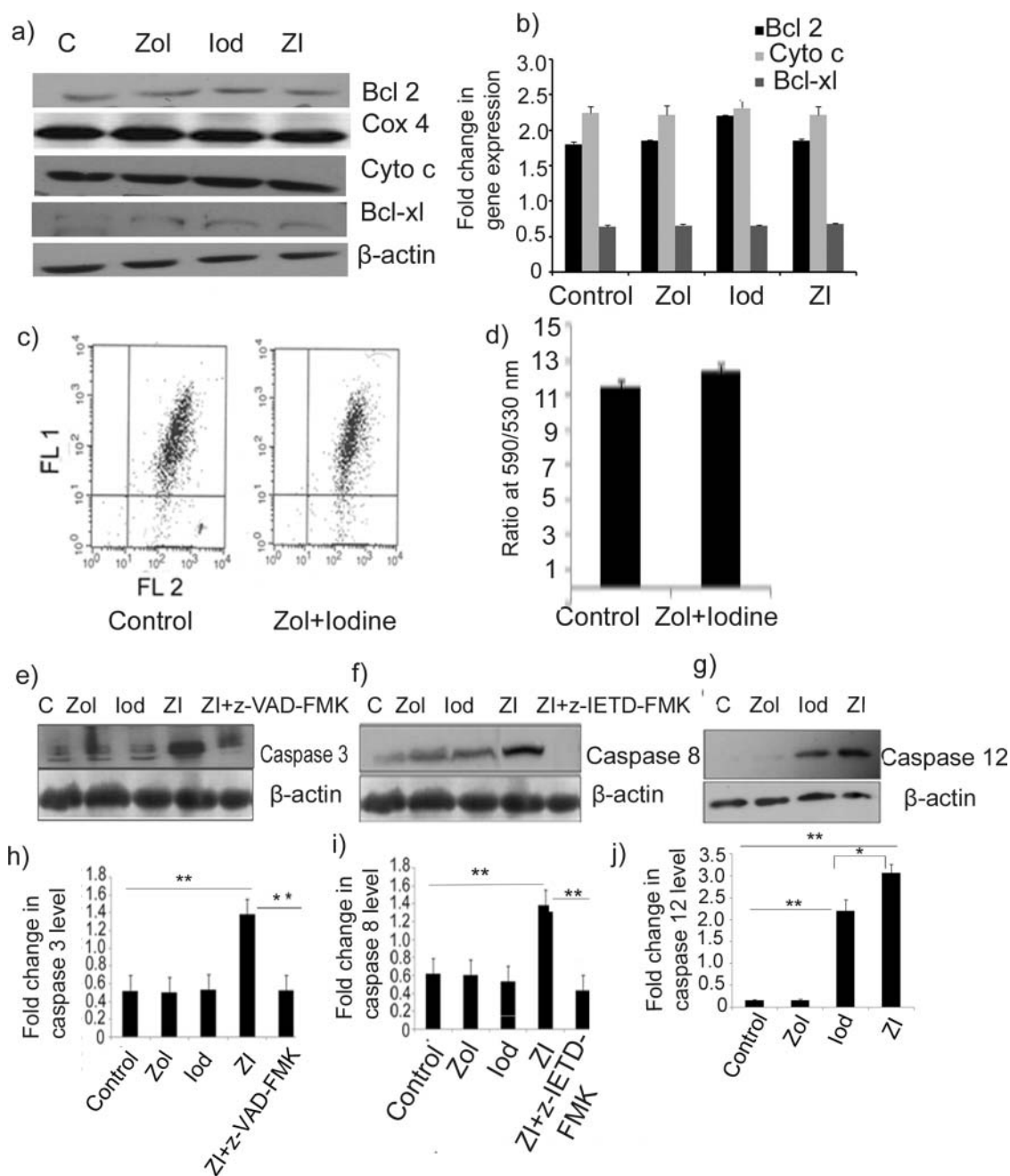


Figure 2. Representative immunoblots of apoptotic markers and flow cytometry for mitochondrial membrane permeability transition. MDA-MB-231 cells were treated with vehicle, Zol, I₂, and Zol+I₂ at concentrations given in experimental design for 48 h. A–B: Representative immunoblot of mitochondrial and whole cell lysate for Bcl 2, cytochrome C, and Bcl-XL. B: Densitometry analysis of Bcl 2, cytochrome C, and Bcl-XL normalized with cyclooxygenase 4 and β -actin, respectively. C–D: Mitochondrial membrane permeability transition was assessed using JC-1 (5 μ M) dye. Cells were acquired through flow cytometer in 530 nm (FL-1) and 590 nm (FL-2). Fluorescence was measured by taking the ratio of 590/530 nm. D: Quantitative analysis of JC-1 fluorescence. E–F: Immunoblot and their histograms of whole cell lysate for cleaved caspase 3 and G–H: caspase 8 expression. In a separate experiment, MDA-MB-231 cells treated with Zol+I₂ were also co-treated with universal caspase inhibitor Z-VAD-FMK (caspase 3) and caspase 8-specific inhibitor Z-1ETD-FMK for 48 h. β -Actin was taken as loading control. I–J: Immunoblot and histogram of whole cell lysate for caspase 12 after the above-mentioned treatment modalities. Values represent the mean \pm SD of triplicate experiments. ** indicates $P < 0.001$ versus control.

Zol+I₂-treated cells by heparin; however, unlike [Ca²⁺]_i, it remained significantly higher relative to vehicle (Fig. 4A and 4B). These findings suggest that ER Ca²⁺ depletion may contribute to apoptosis in MDA-MB-231 cells.

To test this, we measured the ER calcium content with thapsigargin (a stimulator of intracellular Ca²⁺) in the ER lumen. The rise in ER calcium content in response to thapsigargin, in EGTA-pretreated cells, was significantly

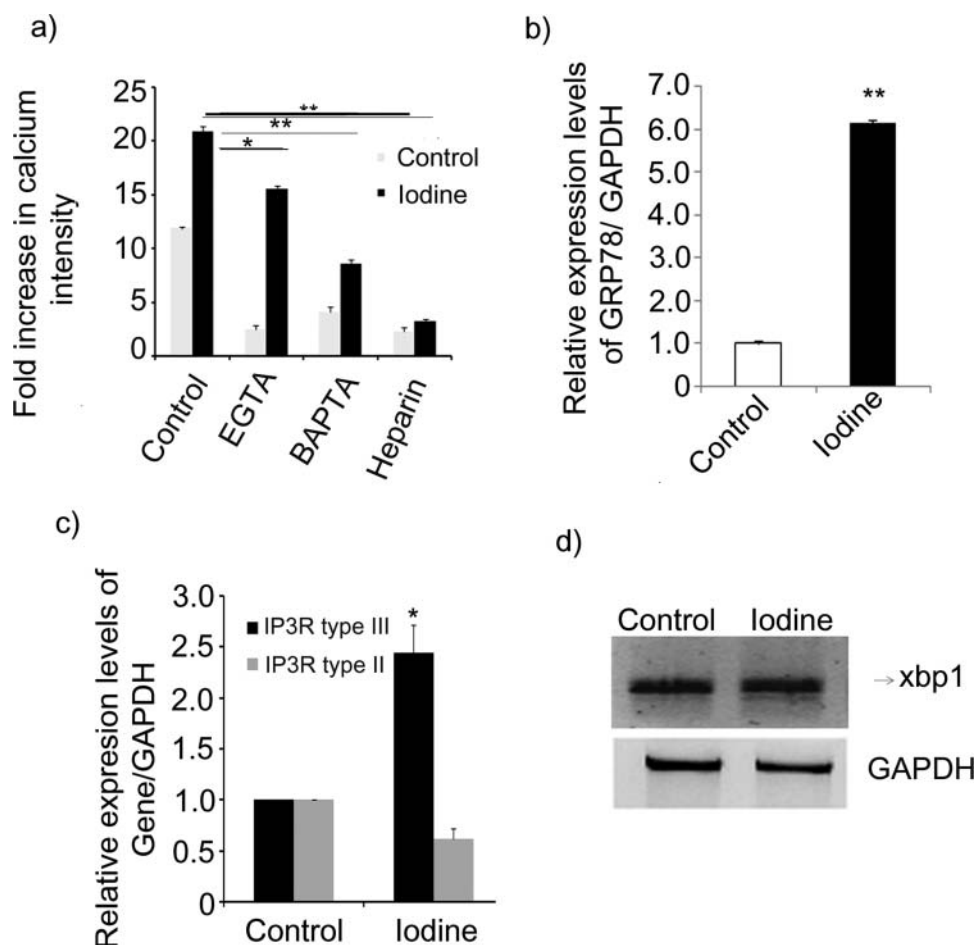


Figure 3. A: MDA-MB-231 cells were pretreated with either 1 mM EGTA for 24 h or 10 μ M BAPTA-AM for 4 h or 5 mg/ml heparin for 12 h, and then treated with either vehicle or I_2 at 2 μ M for 48 h. Free $[Ca^{2+}]_c$ was measured with Oregon green BAPTA-AM at 520 nm (FL-1) by flow cytometry and expressed as fold increase. B–C: Representative histogram showing the relative transcript levels of GRP78, IP3R2, and IP3R3 by real-time PCR. GAPDH was used for normalization. D: Detection of Xbp1 splice variants by electrophoresis on 1.5% agarose of real-time PCR reaction products. Data represent mean \pm SD of triplicate experiment * $P < 0.01$ versus control, ** $P < 0.001$ versus control.

lower in Zol+ I_2 -treated cells compared to vehicle-treated cells (Fig. 4C). Moreover, Zol+ I_2 -treated cells had significantly reduced transcript levels of IP3R2 (fourfold) and IP3R3 (sixfold) relative to vehicle, IP3R1 remained unaltered (Fig. 4D).

To check whether the changes in IP3Rs have any bearing on the apoptotic mechanism, we analyzed the transcript levels of molecular chaperones. A significant increase in the transcript levels of GRP78 and CHOP (Fig. 4E and 4F), protein levels of CHOP (Fig. 4G), and appearance of cleaved Xbp1 at transcript level (Fig. 4H) was observed in Zol+ I_2 -treated cells relative to controls.

Zol+ I_2 reduces mRNA transcript levels of MMP-2 as well as MMP-9

To determine the antimetastatic potential of Zol+ I_2 treatment, we measured the transcripts of MMP-2

and -9. The results indicated that MDA-MB-231 cells harbor high amounts of these proteins (Fig. 5A). We observed a significant fold decrease in mRNA transcript levels of MMP-2 as well as MMP-9 in Zol+ I_2 -treated cells compared to either vehicle-treated cells or cells treated individually either by Zol or I_2 (Fig. 5A). To find whether combination treatment affects invasion potential of MDA-MB-231 cells, migration assays were carried out. The results showed significantly less number of Zol+ I_2 -treated cells migrated to scratched area and also invaded through the collagen-coated chamber relative to vehicle-treated cells (Fig. 5B–E). In addition, the effect of treatment on tumor progression was assessed in mice model of breast cancer. Zol+ I_2 treatment prevented tumor formation and appearance of metastatic nodules in mice lungs (Fig. S2)

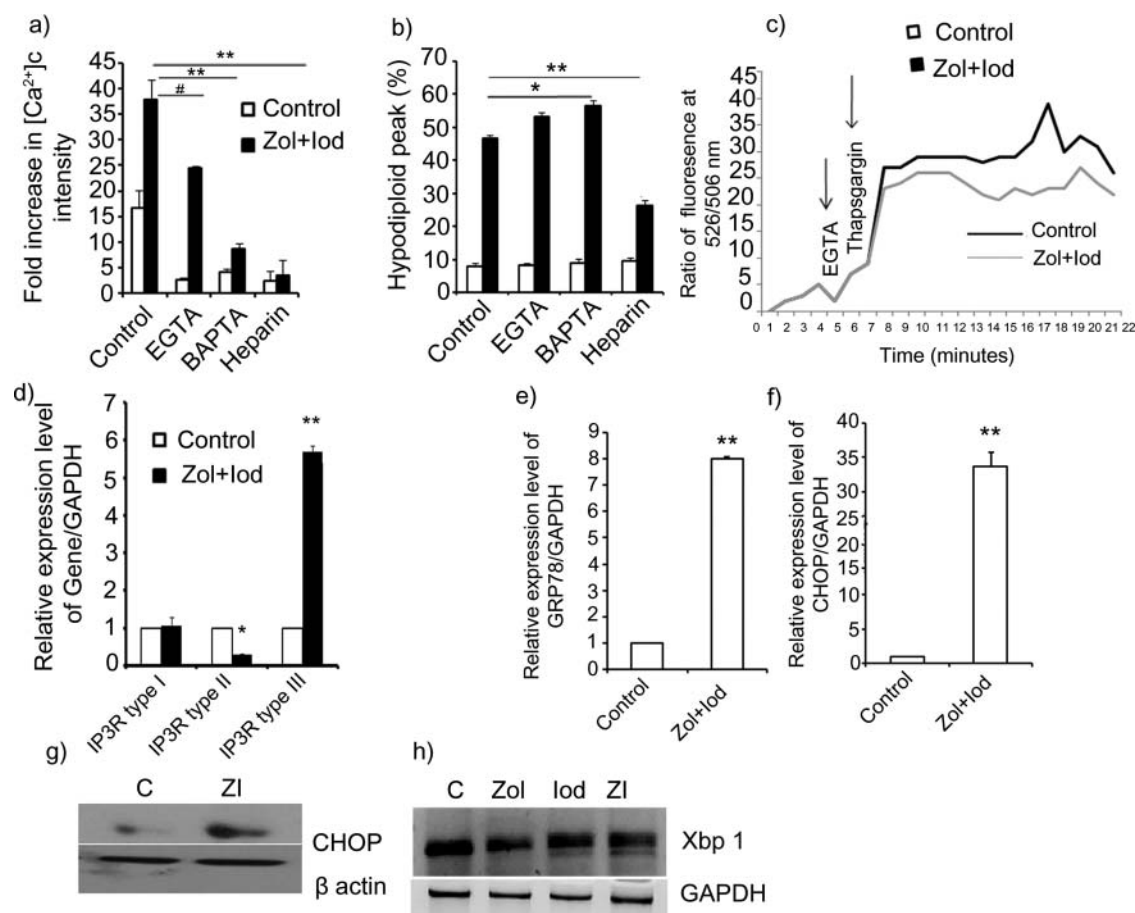


Figure 4. Zol+I₂ induced changes in calcium homeostasis. A: MDA-MB-231 cells were pretreated with vehicle, 1 mM EGTA for 24 h or 10 μ M BAPTA-AM for 4 h or 5 mg/ml heparin for 12 h, and then treated with Zol+I₂ for indicated time period. Free $[Ca^{2+}]_i$ was measured at 520 nm (FL-1) by flow cytometry and expressed as fold increase. B: Apoptosis (hypodiploid peak) using PI staining after 48 h, by flow cytometry. C: Representative fluorimetric analysis of MDA-MB-231 cells treated with Zol+I₂ for 48 h using fluorescence calcium dye Fluo 3-AM dye (526/506 nm). The ratio of emitted fluorescence of Fluo 3-AM was monitored and thapsigargin was added 2 min after pretreatment with 1 mM EGTA. D: Representative histogram showing the relative expression of IP3R1, IP3R2, and IP3R3 by real-time PCR. GAPDH was used for normalization. E–F: Representative histogram showing the relative expression of GRP78 and CHOP by real-time PCR. GAPDH was used for normalization. G: Representative immunoblots of whole cell lysate for CHOP after treatment with Zol, I₂, Zol+I₂, and vehicle (control) H: Detection of Xbp1 splice variants by electrophoresis on 1.5% agarose of real-time PCR reaction products. Data are expressed as the mean of triplicate experiments mean \pm SD of triplicate experiments. # indicates $P < 0.05$ versus control, * indicates $P < 0.01$ versus control, ** indicates $P < 0.001$ versus control.

Discussion

The present study was designed to evaluate the antineoplastic effect of I₂ in conjunction with Zol—the most commonly used antiresorptive adjuvant as pain alleviator of breast tumors. We report that Zol potentiates the efficacy of I₂ by inducing non-mitochondrial intrinsic apoptosis by increasing intracellular calcium and ER stress. We show that MDA-MB-231 cells register minimal hypodiploidy in response to individual treatment with either I₂ or Zol, but synergistically enhances apoptosis when given in combination. Similar potentiating effect as reflected by enhanced apoptotic index on I₂-mediated cell death was also reported in these cells by addition of chloroquine (12) and by addition of doxorubicin in other

animal tumor models and cancer cells (11,19). We had earlier shown the absence of apoptosis and cytotoxicity of I₂ at 4 μ M dose in human peripheral blood mononuclear cells (PBMCs) (10). Bisphosphonates administered intravenously or orally are well tolerated. Nevertheless, cumulative administration of high dosage results in side effects and complications including acute-phase reaction, nephrotoxicity, osteonecrosis of the jaw, and gastrointestinal disturbances. However, very scant information is available so far on the toxicity and safety profile of this marketed drug (31).

The study results show the potentiating effect of Zol on enhancement of apoptosis is not mediated by classical intrinsic mitochondrial-mediated pathway. Combined treatment increased the levels of caspase 8 indicating the

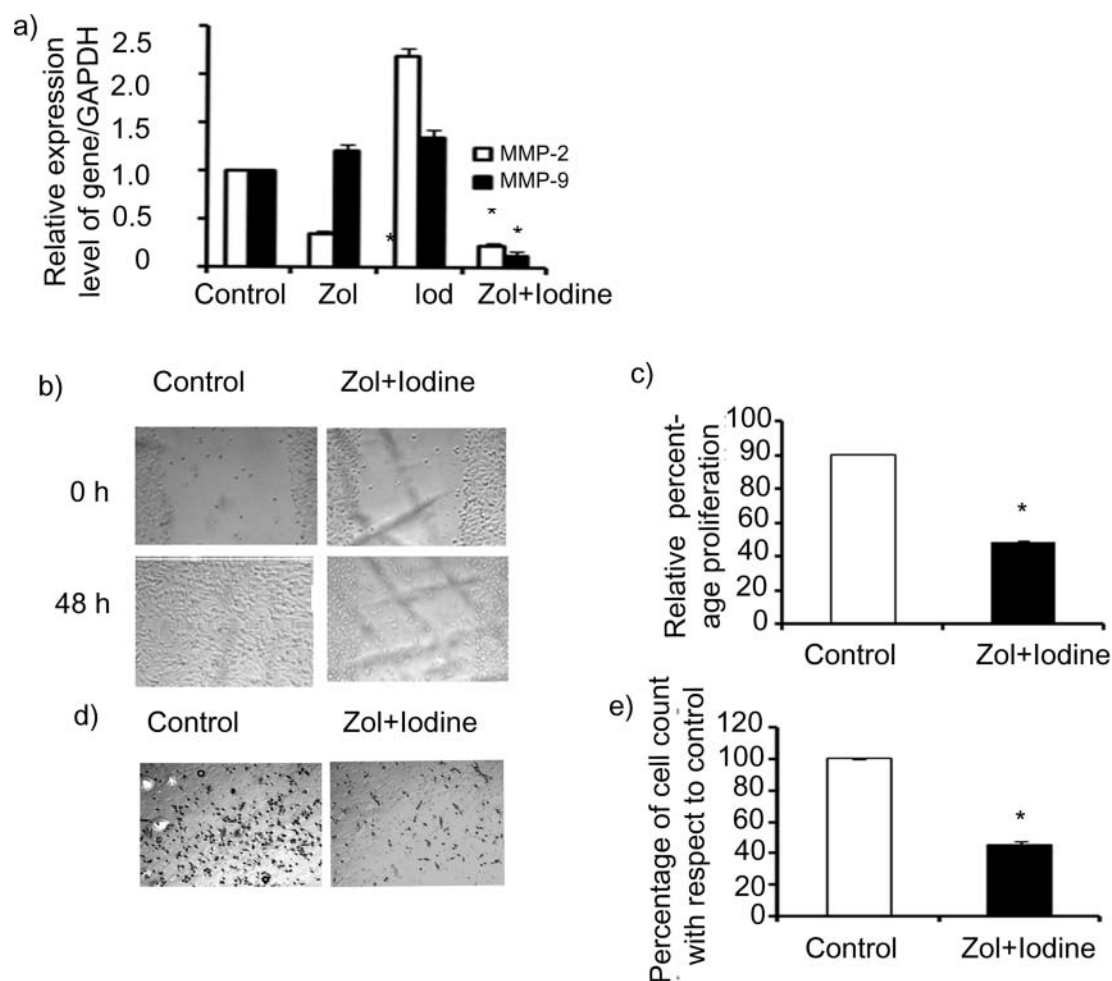


Figure 5. Effects of Zol, I_2 , and Zol+ I_2 on wound-healing assay. After 48-h treatment, each well was examined by phase-contrast microscopy for the amount of wound closure, and the wound images were captured. A: MMP-2 and MMP-9 transcripts in MDA-MB-231 cells by real-time PCR. β -Actin was used as loading vehicle (control) B: Effect of Zol, I_2 , and Zol+ I_2 on invasiveness of MDA-MB-231 cells by wound-healing assay. C: Histogram shows the relative proliferation determined after subtracting the final average wound width. D: Representative phase-contrast image of the cells after methylene blue staining which have migrated the Matrigel were visualized on the lower side of Matrigel membrane. E: Histogram showing the number of cells counted in five different fields; percentage was taken with respect to vehicle (control). Data represent mean \pm SD of three independent experiments. *indicates $P < 0.01$ versus vehicle (control). Note: Vehicle was treated as control.

involvement of extrinsic pathway compared to the constitutive expression of caspase 8 both in untreated as well as I_2 -treated cells. However, the extent of caspase 8 increase alone was not able to explain the synergistic increase in hypodiploidy. This along with iodine's antioxidative effect and Zol's propensity to chelate calcium pointed toward the involvement of ER (20,21). We hypothesized that ER stress might lead to additional apoptotic pathway that could explain the synergistic rise in apoptosis. We first tested and found that caspase 12 located in ER registered increase in both I_2 treatment and significantly more so with combined treatment. In this context, it is important to note that I_2 fails to elicit apoptosis in PBMCs from healthy controls (10) with the near absence of ER stress and calcium homeostatic

perturbation in such cells (27). In contrast, I_2 induces autophagy in triple negative MDA-MB-231 cells and this response seems to be regulated by the enhanced ER stress and perturbation of calcium homeostasis. However, the further enhancement of ER stress and perturbation of calcium homeostasis by combined treatment of Zol+ I_2 leads to significant apoptotic cell death.

To dissect these effects of combined treatment, we first analyzed the effect I_2 alone. We found significantly higher expression of IP3R3 and unaltered levels of IP3R2 when compared with levels of these receptors in untreated cells. Thus, I_2 alone seems to cause increase in intracellular calcium and ER stress. The autophagic action of I_2 on these cells is in agreement with earlier findings that I_2 treatment results in accumulation of

acidic vacuoles and autophagic vacuoles causing autophagosome formation and their vesicular fusion with nucleolus (12). Further I₂ treatment causes splicing of Xbp1 and upregulation of CHOP leading to GRP78 appearance similar to one seen in hepatocellular carcinoma (22). We also observed that autophagy induction event follow ER stress as indicated by earlier appearance GRP78 than LC3 (Fig. S1 D,E).

When cells are co-treated with Zol and I₂ all the parameters including total cellular calcium, IP3R3, GRP78, and Xbp1 cleavage are further significantly increased compared with either untreated cells or cells treated with I₂ alone. To understand the role of enhanced calcium in cells with and without I₂ treatment alone as well as those treated with I₂ and Zol, cells were exposed to various calcium chelators. The exposure of untreated cells to either extracellular chelator EGTA or intracellular chelator BAPTA or IP3R blocker heparin results in highly reduced cytoplasmic calcium levels without apparent elevation of hypodiploidy. In contrast, I₂-treated as well as I₂+Zol-treated cells showed highly elevated cytoplasmic calcium levels decreasing significantly with <EGTA, <<BAPTA, and <<< heparin. This decrease was found to be the highest in I₂+Zol-treated cells exposed to BAPTA that displayed significantly enhanced hypodiploidy. The enhanced cytoplasmic calcium levels were a characteristic gain of I₂+Zol-treated cells. This gain seems to be contributed mainly by intracellular transfer of calcium from ER in consonance with the highest increase seen in calcium chaperons and Xbp1 splicing (23). Lowered stimulatory effect of thapsigargin on EGTA-treated I₂+Zol-exposed cells further strengthens our hypothesis that combined treatment with I₂+Zol creates enormous stress in ER and causes overload of calcium in the interior environment of cells, which try to relieve this through induction of apoptosis plausibly through caspase 12 activation (24–26).

Thus, equipped with enhanced apoptotic mechanism, we further showed the capability of combination treatment to reduce MMP-2 and -9 as well as the reduced migration/invasion potential. The tumor growth arrest in 4T1 mouse model further points toward the possible beneficial use of this combination as adjuvant therapy for breast tumors, especially the triple receptor negative type. The examination of spleen, liver, and heart tissues from Zol+I₂-treated tumor-bearing mice showed no evidence of cellular damage (data not shown), ruling out any adverse effect on other organs. Since both I₂ and Zol have been found to be nontoxic in doses used in the present study, it provides an attractive combination that calls for proving under clinical setting essential to bring potential benefits for patients suffering from triple receptor negative breast cancers. The better iodine nutrition

has been predicted to be helpful for breast cancer prevention. This is emphasized in epidemiological studies published earlier as well as animal studies (27,28,29,5,30). Further, daily consumption of seaweeds like wakame with high I₂ content is more effective than iodate or iodide and is believed to be the cause of the lowest incidence of breast cancer in Japanese women. In this perspective, various studies including the present one (1,2,4,10,12) give credence to the adequacy of iodine nutrition as an essential condition for breast health.

To the best of our knowledge, this is the first report on the potential of I₂ as an adjuvant combination with Zol for the treatment of metastatic breast cancers.

Abbreviations

Bax	(Bcl2-associated X protein)
Bcl2	(B-cell lymphoma 2)
Bcl-XL	(B-cell lymphoma-extra large)
[Ca ²⁺]	(Cytosolic calcium)
Cyto C	(Cytochrome C)
COX4	(Cyclooxygenase 4)
CHOP	(C/EBP homologous protein)
GADD153	(Growth arrest and DNA damage inducible gene 153)
GRP78	(Glucose-regulated protein)
I ⁻	(Iodide)
IP3R1, IP3R2, and IP3R3	(Inositol-1,4,5-triphosphate receptor type 1, type2, and type3)
LC3	(Light chain protein 3)
MMP	(Matrix metalloproteinase)
MPT	(Mitochondrial membrane permeability transition)
ROS	(Reactive oxygen species)
TUNEL	(Terminal deoxynucleotidyl transferase dUTP nick end labeling)
Xbp1	(X-box-binding protein 1)
Zol	(Zoledronate)
Z-IETD-FMK	(Z-Ile-Glu(OMe)-Thr-Asp (OMe)-fluoro methyl ketone)
Z-VAD-FMK	(Z-Val-Ala-Asp-fluoro-methyl ketone)

Funding

This work was supported by the Department of Biotechnology, New Delhi (Grant BT/PR 9822/MED/30/42/2007 to Godbole M M) and research fellowship from the Indian Council of Medical Research, New Delhi (3/2/152/2008/NCD-III to Ranu Tripathi).

References

- Aceves C, Anguiano B, and Delgado G: Is iodine a gate-keeper of the integrity of the mammary gland? *J Mammary Gland Biol Neoplasia* **10**, 189–196, 2005.
- Aceves C, Anguiano B, and Delgado G: The extrathyronine actions of iodine as antioxidant, apoptotic, and differentiation factor in various tissues. *Thyroid* **23**, 938–946, 2013.
- Rosner H, Torremante P, Moller W, and Gartner R: Antiproliferative/cytotoxic activity of molecular iodine and iodolactones in various human carcinoma cell lines. No interfering with EGF-signaling, but evidence for apoptosis. *Exp Clin Endocrinol Diabetes* **118**, 410–419, 2010.
- Venturi S: Is there a role for iodine in breast diseases? *Breast* **10**, 379–382, 2001.
- Funahashi H, Imai T, Tanaka Y, Tsukamura K, Hayakawa Y, et al.: Wakame seaweed suppresses the proliferation of 7,12-dimethylbenz(a)-anthracene-induced mammary tumors in rats. *Jpn J Cancer Res* **90**, 922–927, 1999.
- Garcia-Solis P, Alfaro Y, Anguiano B, Delgado G, Guzman RC, et al.: Inhibition of N-methyl-N-nitrosourea-induced mammary carcinogenesis by molecular iodine (I₂) but not by iodide (I⁻) treatment Evidence that I₂ prevents cancer promotion. *Mol Cell Endocrinol* **236**, 49–57, 2005.
- Stoddard FR, 2nd, Brooks AD, Eskin BA, and Johannes GJ: Iodine alters gene expression in the MCF7 breast cancer cell line: evidence for an anti-estrogen effect of iodine. *Int J Med Sci* **5**, 189–196, 2008.
- Gartner R, Rank P, and Ander B: The role of iodine and delta-iodolactone in growth and apoptosis of malignant thyroid epithelial cells and breast cancer cells. *Hormones (Athens)* **9**, 60–66, 2010.
- Arroyo-Helguera O, Anguiano B, Delgado G, and Aceves C: Uptake and antiproliferative effect of molecular iodine in the MCF-7 breast cancer cell line. *Endocr Relat Cancer* **13**, 1147–1158, 2006.
- Shrivastava A, Tiwari M, Sinha RA, Kumar A, Balapure AK, et al: Molecular iodine induces caspase-independent apoptosis in human breast carcinoma cells involving the mitochondria-mediated pathway. *J Biol Chem* **281**, 19762–19771, 2006.
- Alfaro Y, Delgado G, Carabez A, Anguiano B, and Aceves C: Iodine and doxorubicin, a good combination for mammary cancer treatment: antineoplastic adjuvancy, chemoresistance inhibition, and cardioprotection. *Mol Cancer* **12**, 45, 2013.
- Singh P, Godbole M, Rao G, Annarao S, Mitra K, et al: Inhibition of autophagy stimulate molecular iodine-induced apoptosis in hormone independent breast tumors. *Biochem Biophys Res Commun* **415**, 181–186, 2011.
- Daubine F, Le Gall C, Gasser J, Green J, and Clezardin P: Antitumor effects of clinical dosing regimens of bisphosphonates in experimental breast cancer bone metastasis. *J Natl Cancer Inst* **99**, 322–330, 2007.
- Verdijk R, Franke HR, Wolbers F, and Vermees I: Differential effects of bisphosphonates on breast cancer cell lines. *Cancer Lett* **246**, 308–312, 2007.
- Okada C, and Rechsteiner YM: Introduction of macromolecules into cultured mammalian cells by osmotic lysis of pinocytotic vesicles. *Cell* **29**, 33–41, 1982.
- Ma YG, Liu WC, Dong S, Du C, Wang XJ, et al: Activation of BK(Ca) channels in zoledronic acid-induced apoptosis of MDA-MB-231 breast cancer cells. *PLoS One* **7**, e37451, 2012.
- Roger S, Potier M, Vandier C, Le Guennec JY, and Besson P: Description and role in proliferation of iberiotoxin-sensitive currents in different human mammary epithelial normal and cancerous cells. *Biochim Biophys Acta* **1667**, 190–199, 2004.
- Song SD, Zhou J, Zhao H, Cen JN, and Li DC: MicroRNA-375 targets the 3-phosphoinositide-dependent protein kinase-1 gene in pancreatic carcinoma. *Oncol Lett* **6**, 953–959, 2013.
- Liang X, Tang J, Liang Y, Jin R, and Cai X: Suppression of autophagy by chloroquine sensitizes 5-fluorouracil-mediated cell death in gallbladder carcinoma cells. *Cell Biosci* **4**, 10, 2014.
- Lan YC, Chang CL, Sung MT, Yin PH, Hsu CC, et al: Zoledronic acid-induced cytotoxicity through endoplasmic reticulum stress triggered REDD1-mTOR pathway in breast cancer cells. *Anticancer Res* **33**, 3807–3814, 2013.
- Russell RG, Watts NB, Ebetino FH, and Rogers MJ: Mechanisms of action of bisphosphonates: similarities and differences and their potential influence on clinical efficacy. *Osteoporos Int* **19**, 733–759, 2008.
- Shuda M, Kondoh N, Imazeki N, Tanaka K, Okada T, et al: Activation of the ATF6, XBP1 and grp78 genes in human hepatocellular carcinoma: a possible involvement of the ER stress pathway in hepatocarcinogenesis. *J Hepatol* **38**, 605–614, 2003.
- Verfaillie T, Salazar M, Velasco G, and Agostinis P: Linking ER stress to autophagy: potential implications for cancer therapy. *Int J Cell Biol* 930509, 2010.
- Schonthal AH: Endoplasmic reticulum stress: its role in disease and novel prospects for therapy. *Scientifica (Cairo)* 857516, 2012.
- Shiraishi H, Okamoto H, Yoshimura A, and Yoshida H: ER stress-induced apoptosis and caspase-12 activation occurs downstream of mitochondrial apoptosis involving Apaf-1. *J Cell Sci* **119**, 3958–3966, 2006.
- Zhu Y, Men R, Wen M, Hu X, Liu X, and Yang L: Blockage of TRPM7 channel induces hepatic stellate cell death through endoplasmic reticulum stress-mediated apoptosis. *Life Sci* **94**, 37–44, 2014.
- Eskin BA, Shuman R, Krouse T, and Merion JA: Rat mammary gland atypia produced by iodine blockade with perchlorate. *Cancer Res* **35**, 2332–2339, 1975.
- Eskin BA, Grotkowski CE, Connolly CP, and Ghent WR: Different tissue responses for iodine and iodide in rat thyroid and mammary glands. *Biol Trace Elem Res* **49**, 9–19, 1995.
- Ghent WR, Eskin BA, Low DA, and Hill LP: Iodine replacement in fibrocystic disease of the breast. *Can J Surg* **36**, 453–460, 1993.
- Funahashi H, Imai T, Tanaka Y, Tobinaga J, Wada M, et al: Suppressive effect of iodine on DMBA-induced breast tumor growth in the rat. *J Surg Oncol* **61**, 209–213, 1996.
- Lacerna L, and Hohnaker J: Zoledronic acid for the treatment of bone metastases in patients with breast cancer and other solid tumors. *Semin Oncol* **30**, 150–160, 2003.